ACS Sustainable Chemistry & Engineering

Research Article

pubs.acs.org/journal/ascecg

Raman and NMR Spectroscopic Studies on Hydrolytic Degradation of D,L-Lactide–δ-Valerolactone–D,L-Lactide Copolymer

Nibedita Kasyapi,[†] Radhika Mehta,[‡] and Anil K. Bhowmick*[,§]

[†]Department of Materials Science and Engineering and [‡]Department of Chemistry, Indian Institute of Technology Patna, Patna 800013, India

[§]Rubber Technology Centre, Indian Institute of Technology Kharagpur, Kharagpur 721302, India

Supporting Information

ABSTRACT: Hydrolytic degradation of BAB terpolymers with δ-valerolactone as the central (A) block and D,L-lactide as the terminal (B) block was studied by ^{1}H NMR and Raman spectroscopic techniques. The following variations were investigated: (i) the ratio of δ-valerolactone to D,L-lactide, (ii) replacement of D,L-lactide with cis-lactide or glycolide, keeping A constant, and (iii) replacement of δ-valerolactone with ε-caprolactone, keeping B constant. The intensity of the characteristic peaks for the D,L-lactide segment almost disappeared, and the intensity of the characteristic signals for δ-valerolactone decreased after 30 days. As evident from quantitative analysis of ^{1}H NMR, 97% of the D,L-lactide segment degraded within 30 days, and the value was 35% for the δ-valerolactone block (both based on the initial value). Upon degradation of the triblock, a significant increase in water uptake and decrease in molecular weight and bulk weight were observed. Crystallinity of the triblock increased after degradation due to removal of the amorphous D,L-lactide from the system. An enormous increase in the ΔH_m value after degradation was observed, supporting the increase in crystallinity. Replacing the middle segment with ε-caprolactone resulted in only 0.64% degradation of the middle segment in 30 days. The degradation of terminal segment was reduced using cis-lactide or glycolide in place of D,L-lactide. The disappearance of Raman signal at 870 cm^{-1} assigned for υC–COO stretching of DLL segment along with a decrease in C=O stretching region (1725 cm^{-1}) indicated cleavage of the ester linkages. Lower biodegradability of the triblock containing ε-caprolactone was also apparent from 29% degradation in the C=O region compared to 55% degradation for the triblock with δ-valerolactone. Strong peaks at 1776, 1247, and 996 cm^{-1} were observed after 30 days due to remaining crystalline domains of polyglycolide in the triblock.

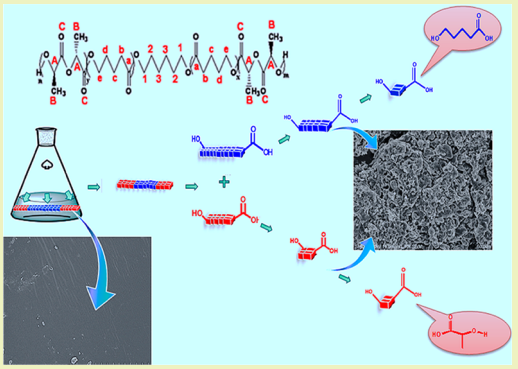

KEYWORDS: *Degradation, NMR, Raman spectroscopy, Biodegradable material, δ-Valerolactone, D,L-Lactide*

INTRODUCTION

In recent years, biodegradability of a polymer appears to be a potential solution for the disposal of synthetic polymers. All of the commodity plastics degrade, but an ecological problem persists due to their longer time span for degradation. Attempts have been made to replace conventional plastics with biodegradable polymers in time-limited applications, such as agricultural packaging material,[1] and in biomedical fields, such as temporary fixation devices, suture materials, tissue engineering scaffolds, and drug delivery vesicles.[2−4] The wide employability of the family of biomaterials from everyday life to state of the art applications, such as tissue engineering, urges scientists to generate new biodegradable materials. Improving homopolymers by blending, copolymerization, and stereopolymerization is worthwhile for adjusting their biodegradation rate and mechanical and physical properties.

Different terminologies have been proposed so far to define polymer breakdown[5] (i.e., biodegradable, bioresorbable, bioerodable, and bioabsorbable) with each degradation phenomenon being different from the others, as described by Huang et al.[6] The degradation process can proceed through macromolecular structure breakdown in vivo with residues being removed from the site of action but not eliminated from the body.

Aliphatic polyesters have been extensively studied because of their degradable labile ester moieties. Most biodegradable polymers reported in the literature are composed of polylactides,[7−9] polylactones,[5,6,10] and polyglycolides[11,12] and a few of their copolymers. Polylactides, especially poly(L-lactide) (PLLA) is widely used as a biomaterial[13] along with poly(D,L-lactide) (PDLLA). Whereas PLLA is crystalline, PDLLA is amorphous and thus has a higher degradation rate than PLLA, making it more suitable for drug delivery and scaffolding purposes. Polylactides are known to undergo hydrolytic degradation via bulk erosion following scission of an ester linkage. The degradation product lactic acid is a human

Received: February 16, 2015
Revised: April 21, 2015
Published: May 12, 2015

DOI: 10.1021/acssuschemeng.5b00121
ACS Sustainable Chem. Eng. 2015, 3, 1381−1393

Table 1. Sample Details[a]

Sample	Chemical structure	Molecular weight (M_n) Dalton	A:B ratio (from ^{1}H NMR)
$DLL_{17}DV_{66}DLL_{17}$		11000	78:22
$DLL_{10}DV_{80}DLL_{10}$	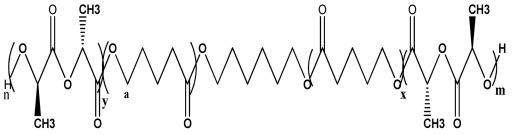	10600	90:10
$DLL_{17}EC_{66}DLL_{17}$	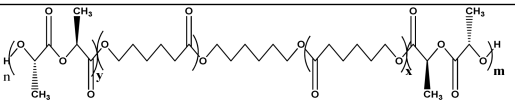	7690	75:25
$CL_{17}DV_{66}CL_{17}$	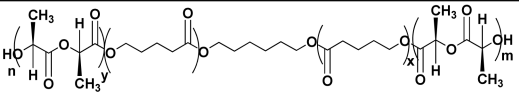	8414	75:25
$GL_{17}DV_{66}GL_{17}$	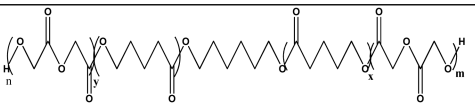	6845	69:31

[a]The weight ratio of monomers incorporated in the triblock, determined by analyzing ^{1}H NMR spectra, was different from the weight ratio of the monomers in the feed composition.

metabolic product that thereafter breaks down to water and carbon dioxide through the citric acid cycle.[13] However, poor elasticity and low drug permeability of polylactides lead to its copolymerization with glycolides or lactones, especially ε-caprolactone.[6,14,15]

Block copolymers of lactide and glycolide-poly lactide-co-glycolide (PLGA) are used in drug delivery systems in the form of microspheres, nanospheres, and nanofibers.[11,16,17] High rate of degradability owing to lactide and glycolide blocks and good cell adhesion makes them suitable for bioapplications. PLGA is shown to degrade via bulk erosion through hydration followed by hydrolysis of ester bonds.[13,18] Their brittleness and quick degradation limit their use in tissue engineering. The use of other lactones in the polymer matrix has also been researched, the most common of which being poly ε-caprolactone.

Poly ε-caprolactone (PCL) has been employed largely in tissue engineering due to its excellent biocompatibility, high permeability, and low preparation costs. However, its slow degradation poses a problem for applications in drug delivery. Thus, it has been copolymerized with lactides, especially PLLA and PDLLA, to improve the properties of the synthesized copolymer for various bioapplications.[6,13,14] To improve its degradability in vitro, PCL has also been copolymerized with δ-valerolactone, which has one less methylene carbon.[19] Thus, like poly ε-caprolactone copolymers, poly δ-valerolactone (DV) copolymers can be well-suited for biological applications, including drug delivery and tissue engineering. However, investigations on poly δ-valerolactone are few and far between. Previous studies on the degradation of δ-valerolactone copolymers are extremely limited,[20] and none of them discussed the same terpolymers. Also, degradation behavior of the polymers with reference to microstructure of the copolymers has not been studied. Furthermore, there is a scope to work on the structure−degradation relationship of the polymers. Such studies on various nonbiodegradable polymers have been reported from our laboratory.[21−24]

Recently, we synthesized and characterized a series of terpolymers (BAB) from δ-valerolactone (A), D,L-lactide (B), ε-caprolactone (A), glycolide (B), and cis-lactide (B).[25,26] This paper deals with the hydrolytic degradation of these terpolymers to establish their acceptability as a drug delivery system. Herein, their degradation with respect to time and

DOI: 10.1021/acssuschemeng.5b00121
ACS Sustainable Chem. Eng. 2015, 3, 1381−1393

composition variation is evaluated. As stated previously, degradation studies of DV- and PDLLA-based triblocks have not previously been performed. The effect of the change on degradation in the terminal block and mid segment is also highlighted in this work.

Thus, this work documents the hydrolytic degradation of terpolymers (BAB) based on δ-valerolactone (A) and D,L-lactide (B) synthesized block terpolymers with respect to time up to 30 days. This time scale is important for understanding the biodegradation pattern and is imperative for any polymer to be employed in a biomedical application. The degradation profile with reference to variation of the lactide ratio is also reported. Finally, a comparison of the degradation behavior of various terpolymers (i.e., replacement of D,L-lactide with cis-lactide or glycolide keeping A constant and replacement of δ-valerolactone with ε-caprolactone keeping B constant) has been made to determine a more suitable composition for bioapplications. To the best of our knowledge, this is the first such study to be reported in the literature.

EXPERIMENTAL SECTION

The polymers $DLL_{17}DV_{66}DLL_{17}$, $DLL_{10}DV_{80}DLL_{10}$, $DLL_{17}EC_{66}DLL_{17}$, $GL_{17}DV_{66}GL_{17}$, and $CL_{17}DV_{66}CL_{17}$ were prepared by ring opening polymerization as reported previously.[25,26] Their chemical structure and molecular weight are given in Table 1. Sodium dihydrogen phosphate, disodium hydrogen phosphate, sodium chloride, and potassium chloride for buffer preparation were obtained from Merck (Germany). Tehtrahydrofuran (HPLC grade) for GPC was obtained from SRL Laboratories (India).

The polymers were molded into pellets using a hydraulic press for the degradation study. Each sample weighing ∼50 mg (m_o) was added to a glass bottle containing 5 mL of 20 mM phosphate buffer saline (pH 7.4), thereby keeping the concentration at 10 mg/mL.

Analysis of Degradation. The measured amount (m_0) of the sample for the degradation study was kept in the buffer solution in a glass bottle, and the assembly was placed in an incubator at 37 °C for 8, 15, and 30 days for $DLL_{17}DV_{66}DLL_{17}$ and for 30 days for all of the other samples.

After degradation, the samples were removed from the incubator, weighed (m_w), and then dried under vacuum for 48−72 h at 40 °C and weighed again (m_d).

The loss of sample due to degradation of the polymer was calculated in accordance with a previous report[7] using

$$\text{sample weight loss (\%)} = \frac{(m_o - m_d)}{m_o} \times 100\% \quad (1)$$

where m_o and m_d are the initial and final dried weights of the degraded polymer sample, respectively.

The water uptake characteristics of the polymer were also observed., and the percentage water uptake[7] was calculated as

$$\text{water uptake (\%)} = \frac{(m_w - m_d)}{m_d} \times 100\% \quad (2)$$

where m_w and m_d are the weights of the degraded polymer before and after drying, respectively.

Raman Spectroscopy. The samples before and after degradation in dried powder form were analyzed by Raman spectroscopy using an STR 750 series (Seki Technotron/Technos Instrument, India) Raman spectrometer with a 633 nm He−Ne laser source and a grating of 600 lines per mm. The laser was focused on a specific area of the sample using a 50× objective lens attached to an optical microscope (Olympus BX-51). The degradation of a particular functional group was calculated using the equation

$$\text{\% degradation of C=O stretching} = \frac{(I_{\text{C=O pristine}} - I_{\text{C=O after degradation}})}{I_{\text{C=O pristine}}} \times 100 \quad (3)$$

NMR Spectroscopy. ^{1}H NMR spectra of the samples before and after degradation were recorded in a model AVANCE III 400 Ascend Bruker operating at 400 MHz. The samples for NMR were prepared in $CDCl_3$ solution, and chemical shifts were reported in δ (ppm) relative to the ^{1}H signals from protic solvent (7.26 ppm for $CDCl_3$). The quantitative analysis from ^{1}H NMR was carried out by calculating the molecular weight of each of the block segments from the intensities of the characteristic protons with respect to signal at δ = 3.6−3.7 ppm for terminal methylene protons of the initiator. The following equation was used to estimate the change in molecular weight of the D,L-lactide segment with respect to the intensities of the methine protons at 5.1 ppm.

$$\text{\%change in molecular weight of D,L-lactide} = \frac{(M_{w(\text{CH pristine})} - M_{w(\text{CH after degradation})})}{(M_{w(\text{CH pristine})})} \times 100 \quad (4)$$

Similarly, the molecular weight loss for the δ-valerolactone segment was calculated from the intensities of the methylene protons appearing at 4.2 ppm.

FTIR Spectroscopy. The FTIR spectra were recorded on KBr pellets using PerkinElmer Spectrum 400 machine in a spectral range of 4000−530 cm^{-1} with a total of 16 scans per sample.

Wide Angle X-ray Diffraction Analysis. Wide angle X-ray diffraction (WAXD) analysis was carried out using a Rigaku TT RAX 3XRD machine with Cu Kα (0.154 nm) as a radiation source at 50 kV. The crystallinity was calculated from peak area analysis, and crystallite size was calculated from the instrument software.

Differential Scanning Calorimetry Analysis. Differential scanning calorimetry (DSC) was conducted in a PerkinElmer DSC8000. Samples, in hermetically sealed aluminum pans, were analyzed using the following steps: the samples were equilibrated at 80 °C at 10 °C/min, cooled to −80 °C at 10 °C/min, followed by reheating to 80 °C at 2 °C/min. The glass transition temperature was reported in the second heating cycle.

Gel Permeation Chromatography Analysis. The molecular weight distribution of the copolymers before and after degradation was measured by an Agilent PLGPC 50 integrated using PLgel 5 μm Mixed-D column equipped with a refractive index detector using THF as the solvent.

Scanning Electron Microscopy (SEM) Analysis. The surface morphology of the samples was examined under a FESEM (Hitachi, S-4800 FESEM) at an accelerating voltage of 10 kV. The pellets of pristine and degraded samples were placed on double sided carbon adhesive tape adhered on the stub and coated with platinum using a Hitachi E-1010 Ion Sputter system.

RESULTS AND DISCUSSION

The synthesized terpolymer $DLL_{17}DV_{66}DLL_{17}$ was subjected to hydrolytic degradation in 20 mM PBS (pH 7.4) over a time period of 30 days. Postdegradation, the samples were evaluated to determine changes in structural properties with the help of Raman, infrared, and nuclear magnetic resonance spectroscopy and also from weight loss, water uptake, molecular weight change, differential scanning calorimetry chromatograms, and SEM. The results of these studies are documented below.

Sample Weight Loss and Water Uptake Profile. The weight loss profile due to degradation of $DLL_{17}DV_{66}DLL_{17}$ in PBS, as calculated using eq 1, is shown in Figure 1. The weight loss in the buffer was seen to increase with time, and the aliquots were observed to turn cloudy. There was weight loss of

DOI: 10.1021/acssuschemeng.5b00121
ACS Sustainable Chem. Eng. 2015, 3, 1381−1393

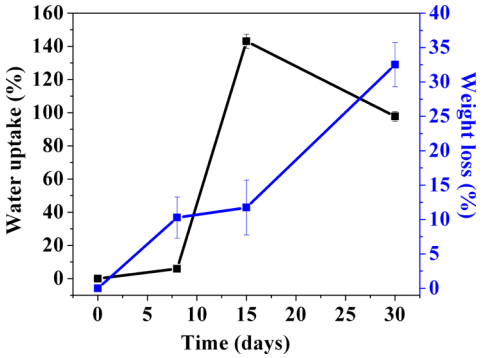

Figure 1. Weight loss and water uptake profile for $DLL_{17}DV_{66}DLL_{17}$ at different time intervals of degradation in 20 mM PBS (pH 7.4).

32% upon immersion of the sample in PBS solution for 30 days.

The water uptake of the terpolymer was plotted as a function of time using eq 2. As shown in Figure 1, the water uptake of the triblock was observed to increase slowly in the initial stage and then increased drastically up to 15 days. This may be attributed to the inherent hydrophobic nature of the triblock. The methyl groups of the terminal D,L-lactide segment initially retarded the penetration of water within the polymer.[27] Then, the water molecules penetrated into the amorphous region of the semicrystalline polymer with a steady increase in water uptake after 8 days. After entry of the water molecules, chain scission occurred preferably in the amorphous region, forming lower molecular weight fragments that were slowly dissolved and favored the diffusion of water molecules in the polymer network.[10] This process showed a drastic increase in water uptake (143%) after 15 days. Upon removal of the amorphous region, the remnant crystalline polymer network inhibited the water penetration, reflecting a decrease in the water uptake (97%) after 30 days. These are substantiated by the crystallinity data and the nature of the fragments produced during degradation.

The degradation is hypothesized to occur due to local changes in pH of the bulk solution due to the formation of acidic moieties and a concentration gradient.[27] This is supported by the fact that the pH of the buffer solution after 8, 15, and 30 days was observed to be 7.4, 7.0, and 6.5, respectively. This slow degradation in buffer over time is very useful, as it is a requirement that the polymer degrades over time and the products formed thus be removed slowly thereafter.

There will be molecular weight loss due to degradation, which is discussed in the section on NMR analysis.

Structural Changes after Degradation. *Raman Spectroscopy.* The degradation profile at different time intervals for $DLL_{17}DV_{66}DLL_{17}$ was monitored by Raman spectroscopy as shown in Figure 2. The characteristic peak for C═O stretching appeared at 1726 cm^{-1}, and the intensity decreased over time. After 30 days, the comparison of peak area at the C═O region showed that 55% of carbonyl was destroyed, indicating ester bond cleavage. The CH/CH_3 stretching in the region 2856–2976 cm^{-1} exhibited multiple signals at 2873, 2924, and 2950 cm^{-1}, confirming the presence of DV and DLL segments. Forty-one percent of the CH/CH_3 groups was degraded within the 30 day interval, as estimated from the peak area. The signals at 1422 and 1457 cm^{-1} for δ $-CH_2$ bending, at 1296 cm^{-1} associated with low intensity signal, at 1260 cm^{-1} for ω-CH_2 wagging, and at 1100 and 1046 cm^{-1} for skeletal stretching, representing the presence of the δ-valerolactone (DV) segment. The signal for asymmetric CH_3 deformation of the D,L-lactide segment overlapped with the signal at 1457 cm^{-1} for δ-valerolactone. A gradual decrease in intensity of the representative signals was noticed within the degradation period, indicating degradation of the DV segment. Quantitatively, the degradation was determined by ^1H NMR spectra, as discussed later. The signal at 870 cm^{-1} assigned to the υC–COO stretching of the DLL segment almost disappeared after 30 days, providing evidence of the degradation of the DLL segment.

IR Spectroscopy. The FTIR spectrum of $DLL_{17}DV_{66}DLL_{17}$ evaluated at time intervals of 8, 15, and 30 days in 20 mM PBS (pH 7.4) is shown in Figure S1 (Supporting Information). The signal for carbonyl stretching showed a bimodal peak in the case of the pristine sample (i.e., one peak around 1762 cm^{-1}) assigned for the carbonyl group of the D,L-lactide segment and another at 1732 cm^{-1} for the δ-valerolactone segment,[25] but after degradation, only the peak at 1728 cm^{-1} was observed, signifying the fact that the block structure was disrupted. The low intensity peak at 1762 cm^{-1} disappeared after 8 days of degradation. This disappearance emphasized the removal of the D,L-lactide segment from the system, but due to overlap of signals of D,L-lactide and δ-valerolactone, it was difficult to determine the extent of degradation of δ-valerolactone using FTIR. Thus, degradation of both the segments was supported quantitatively by ^1H NMR analysis, as discussed below. The

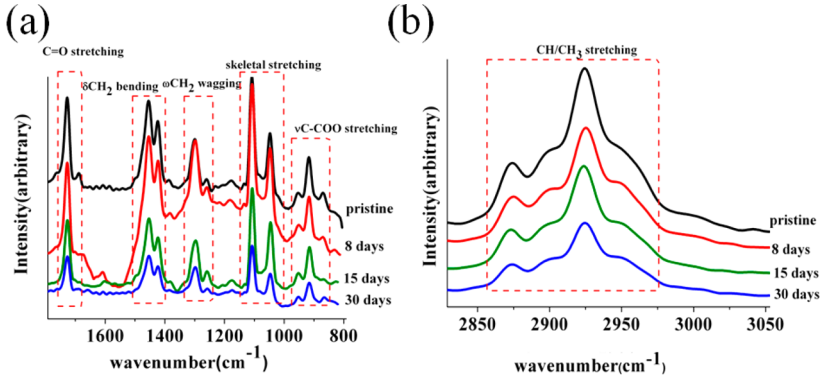

Figure 2. Raman spectra of $DLL_{17}DV_{66}DLL_{17}$ after degradation in 20 mM PBS (pH 7.4) at different time intervals at (a) 800–1800 cm^{-1} and (b) 2830–3050 cm^{-1}.

DOI: 10.1021/acssuschemeng.5b00121
ACS Sustainable Chem. Eng. 2015, 3, 1381–1393

peak area for C═O stretching for the pristine sample calculated as 5705 was reduced to 5096 after 15 days and 3060 after 30 days of degradation in buffer. Thus, biodegradation occurred by hydrolytic chain cleavage of the polyester linkages.

Analysis of FTIR spectra (Figure S2, Supporting Information) of the buffer solution collected after 15 and 30 days showed representative peaks for C−O single bonds at 1129, 1089, and 1038 cm^{-1}, C−H bending at around 1405 cm^{-1}, C═O stretching at 1654 cm^{-1}, and a broad region from 3599 to 2996 cm^{-1} for OH stretching. The appearance of the signals in buffer medium confirmed that the soluble residue was generated by defragmentation of the D,L-lactide segment or the δ-valerolactone segment, and the upfield shift of the C═O stretching from 1730 to 1654 cm^{-1} supported the formation of acid homologues. This was further supported by the pH values. An increase in peak area of the signals was observed after 30 days.

NMR Spectroscopy. Figure 3 demonstrates the ^{1}H NMR spectra of $DLL_{17}DV_{66}DLL_{17}$ taken at different time intervals

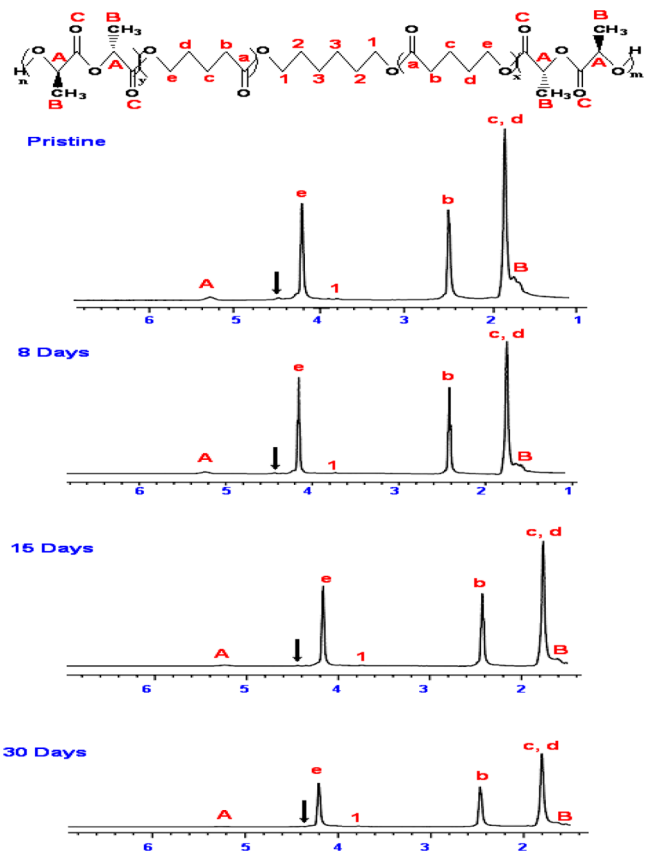

Figure 3. ^{1}H NMR spectra of $DLL_{17}DV_{66}DLL_{17}$ after degradation in 20 mM PBS (pH 7.4) at different time intervals with the black arrow designating a signal at δ = 4.3 ppm.

after degradation in 20 mM PBS at pH 7.4. The representative protons of D,L-lactide segment appeared at δ = 5.2 ppm for methine protons (A) and at δ = 1.5 ppm for methyl protons (B). There was a gradual decrease in intensity of methine protons (δ = 5.2 ppm) and methyl protons (δ = 1.5 ppm) of D,L-lactide segment with time, which almost disappeared after 30 days of degradation. A signal at δ = 4.3 ppm (designated by a black arrow in Figure 3), assigned for the D,L-lactide chain end, also disappeared over time, indicating that all poly D,L-lactide segments were degraded. The molecular weight determination (Figure 4a) from the intensities of the methine protons of D,L-lactide at δ = 5.2 ppm (A) and the terminal methylene protons of 1,6-hexanediol initiator at 3.6 ppm also supported that the molecular weight of the D,L-lactide segment was lowered by 44% after 8 days from its initial value. Ninety-seven percent of the DLL segment was degraded after 30 days. The complete removal of the poly D,L-lactide segment after 30 days was also apparent from the Raman spectra. These might be converted to the monomer (i.e., lactic acid; as shown in Scheme 1). Lactic acid, being soluble in buffer medium, was removed from the polymer system and thus showed no signal in the NMR spectrum of $DLL_{17}DV_{66}DLL_{17}$ after 30 days of degradation. For the δ-valerolactone segment, signals were assigned at δ = 4.2 ppm for methylene protons (e) adjacent to acyl oxygen, at δ = 2.3 ppm for methylene protons attached to carbonyl group (b), and at δ = 1.7 ppm for two internal methylene protons (c, d). All of the peaks for the δ-valerolactone segment were clearly visible even after 30 days. A quantitative analysis of molecular weight (Figure 4a) of the poly δ-valerolactone segment measured from characteristic peak intensities at 4.2 ppm and at 3.6 ppm for terminal methylene protons of initiator 1,6-hexanediol as an internal reference revealed that 7% of its initial weight had been degraded after 8 days, and the value reached 35% after 30 days. The formation of an acidic moiety was proven by FTIR analysis of the buffer medium after different time intervals (Figure S2, Supporting Information) and lowering of the pH from 7.4 to 6.5 after 30 days. If the biodegradation period was extended beyond 30 days, the remaining poly δ-valerolactone segment would be fully degraded to form 5-hydroxypentanoic acid (structure shown in Scheme 1). Initially, the triblock contained approximately 22:78 of D,L-lactide/δ-valerolactone by weight ratio, which was gradually reduced to 9:91 after 8 days, 5:95 after 15 days, and finally to 0.64:99.35 after 30 days. The decrease in lactide ratio from 22 to 5 by weight explained the drastic increase in water uptake after 15 days, and the subsequent decrease in water uptake after 30 days was due to the crystalline nature of the remaining poly δ-valerolactone segment. The crystalline nature of the degraded triblock was evident from WAXD and DSC thermograms, as discussed later. A comparison of the molecular weights determined from NMR and GPC for the corresponding triblock (Figure 4b) demonstrated that, after 8 days, the molecular weight loss was 15% as estimated by ^{1}H NMR but 43% by GPC, which remained almost constant even after 30 days. On the other hand, the molecular weight loss profile from ^{1}H NMR analysis displayed a gradual decrease over the 30 day time period. Such a difference in the molecular weight between ^{1}H NMR and GPC arises because GPC is an indirect method for measuring molecular masses,[28,29] and the macromolecules of the triblock were separated based on differences in their hydrodynamic volumes. There was a significant shift in molecular weight distribution curves after 8 days; later, degradation proceeded with little shift in the retention time (Figure S3a, Supporting Information).

The methine protons, methylene protons, and methyl protons in ^{1}H NMR can be correlated with CH/CH_3 stretching of the Raman spectrum. The decrease in the intensity of the signals obtained from ^{1}H NMR and Raman was measured quantitatively for $DLL_{17}DV_{66}DLL_{17}$. As shown in Figure 5, the degradation calculated from Raman was higher than that

DOI: 10.1021/acssuschemeng.5b00121
ACS Sustainable Chem. Eng. 2015, 3, 1381−1393

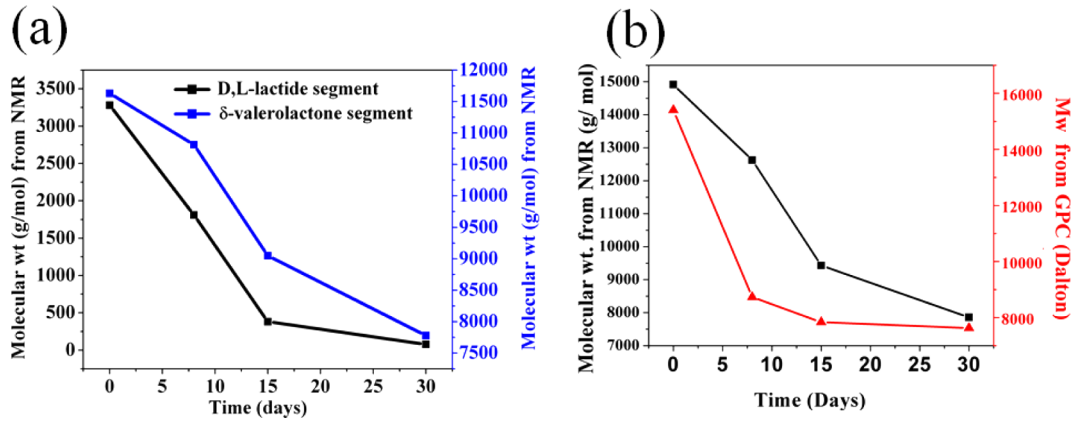

Figure 4. (a) Composition of the terpolymer as a function of degradation time as determined by ^{1}H NMR. (b) Plot of the molecular weight as a function of degradation time from ^{1}H NMR and GPC.

Scheme 1. Degradation Mechanism of D,L-Lactide–δ-Valerolactone–D,L-Lactide Triblock in PBS (pH 7.4)

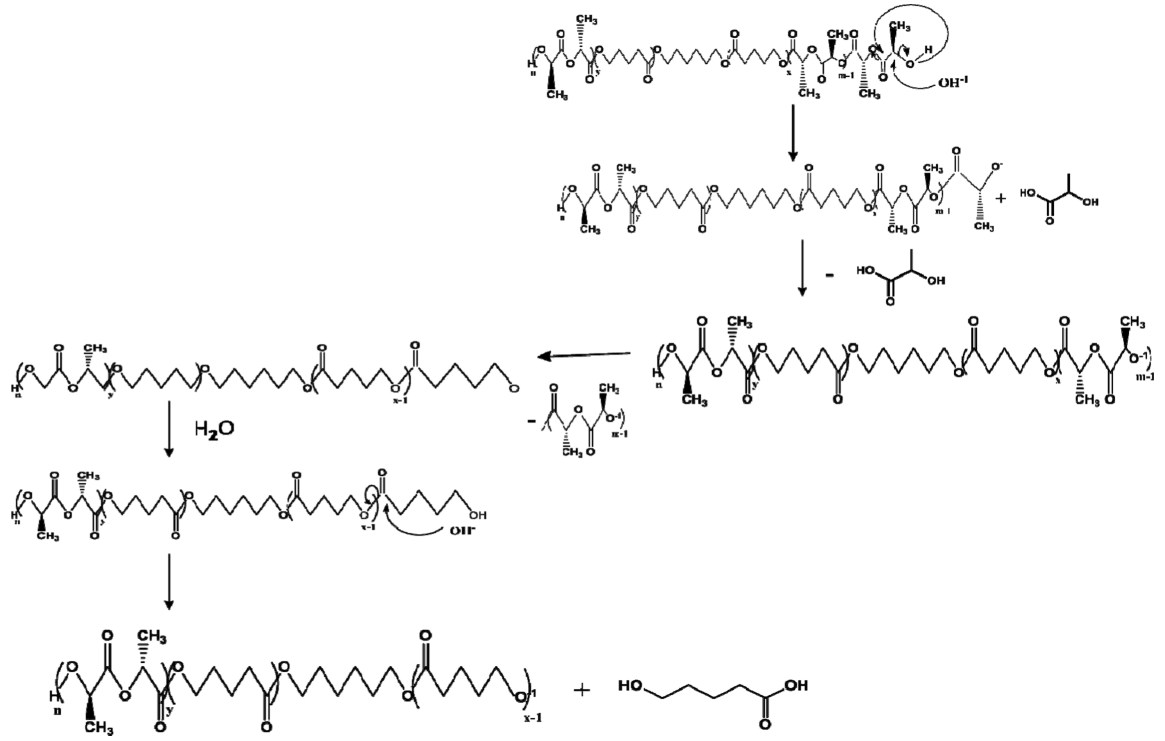

calculated from ^{1}H NMR, but in the initial stage of degradation, the value was in close proximity. The difference in values in ^{1}H NMR and Raman spectra arises due to the fact that, for ^{1}H NMR, the experiments were performed in the solution state whereas capturing the Raman spectrum used the powder form of the sample.

WAXD Analysis. The WAXD analysis (Figure 6) of degraded samples of $DLL_{17}DV_{66}DLL_{17}$ exhibited a major peak at 21.7° associated with a low intensity peak at 24.3° and a small peak at 30.5°, confirming the semicrystalline nature of the triblock. The degradation of the triblock can be explained by measuring the crystallinity parameters over time. As the degradation proceeded, the crystallinity of the triblock inceased from 20% to 47%, and the crystallite size also decreased from 290 Å to 185 Å after 15 days. The increase in crystallinity was due to removal of the amorphous region (i.e., D,L-lactide) from the system. It was also ascertained from ^{1}H NMR analysis that after 15 days the major degradation occurred for D,L-lactide, as the molecular weight of the D,L-lactide segment was reduced by 88%.

Thermal Property Changes. The results described above were further confirmed by the change in thermal properties. The DSC results of $DLL_{17}DV_{66}DLL_{17}$ after 0, 8, 15, and 30 days are shown in Table 2. All of the samples showed two glass transition temperatures (Tg_1 for poly δ-valerolactone and Tg_2 for poly D,L-lactide) characteristic for typical block copolymers as tabulated in Table 2. Tg_1 was observed around −54 °C, whereas Tg_2 was at 7 °C. The glass transition temperature of the terpolymer was seen to vary between −50 and −55 °C for the δ-valerolactone segment with increasing value at 30 days of degradation, whereas the change in Tg_2 for the D,L-lactide segment up to 15 days was not so prominent. No glass transition temperature for the D,L-lactide segment (Tg_2) was detected after 30 days.

DOI: 10.1021/acssuschemeng.5b00121
ACS Sustainable Chem. Eng. 2015, 3, 1381−1393

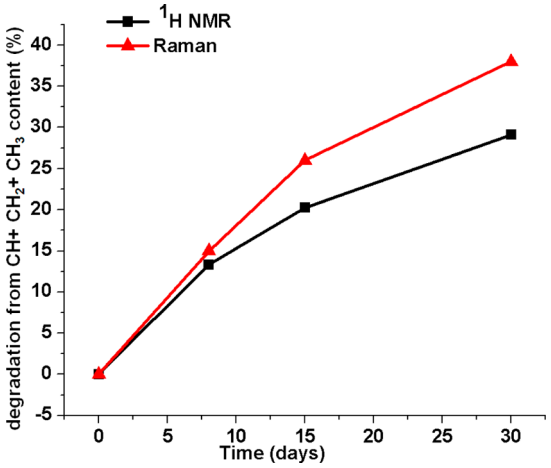

Figure 5. Plot of degradation of total CH+CH$_2$+CH$_3$ content over time as determined by ^{1}H NMR and Raman analysis.

However, there was an apparent shift in the melting temperature of the terpolymer after degradation (Figure S4, Supporting Information). A broad bimodal peak was observed for the pristine terpolymer owing to the broad distribution of crystallite size that sharpened to a single peak upon degradation. Sharpening of the melting peak indicated removal of the amorphous regions from the copolymer (i.e., preferably the D,L-lactide segment), as already supported by ^{1}H NMR and WAXD analysis. The two melting peaks around 48 °C (broad) and 51 °C showed a significant change with a single peak at 52 °C after 8 days. Upon degradation after 15 days, a broad peak at 54 °C was observed. The sample after 30 days of degradation yielded a sharp peak centered around 55 °C.

The ΔH_m showed a drastic increase from 19.07 J/g to 57.7 J/g after 8 days of degradation, which reflects the fact that there was enhanced crystallization ability due to the removal of imperfections or amorphous segments from $DLL_{17}DV_{66}DLL_{17}$. The ΔH_m increased sharply from 57.7 J/g to 100.0 J/g at 30 days. Observations from DSC further supported the results from NMR that the D,L-lactide segment degraded faster than δ-valerolactone.

Imaging via SEM. The $DLL_{17}DV_{66}DLL_{17}$ terpolymer was imaged using SEM after hydrolytic degradation to determine changes in surface morphology with time. As seen in Figure S5a–c in the Supporting Information, there was a significant change in the morphology after 15 and 30 days that confirmed that the synthesized terpolymer was readily degraded in buffer. Panels d and e in Figure S5 in the Supporting Information showed the cross-section of the pellets of pristine and degraded sample after 30 days, which demonstrated that there was degradation internally as well, and it was not limited to erosion of the polymer surface. Initially, the surface of the pellet was smooth, but after 15 days of degradation, the roughness of the surface increased and granules along with large, brighter domains appeared on the surface. The brighter domains were separated from the granules by well-distinguished boundaries. The boundaries between these zones were composed of amorphous region,[30] mainly poly D,L-lactide or crystalline defects, which degraded preferentially. After 30 days, surface erosion resulted in formation of pores on the surface, and bright granules were lying on the surface. The hole formation on the surface was due to removal of poly D,L-lactide segments, as was evident from NMR analysis. The remaining matrix mainly consisted of crystalline poly δ-valerolactone. The morphology of the cross-section was initially rough with the presence of granules and splits, but after 30 days, it appeared as a spongelike structure with clustered particles.

Table 2. Thermal Parameter Changes upon Degradation over Time

	time (days)			
	0	8	15	30
Tg_1 (°C)	−54.0	−55.0	−50.0	−51.0
Tg_2 (°C)	7.0	7.0	7.5	
T_m (°C)	47.7 and 51.5	52.0	53.5	55.0
ΔH_m (J/g)	19.0	57.7	68.9	100.0

Monomer Ratio Variation. The ^{1}H NMR spectra of $DLL_{10}DV_{80}DLL_{10}$ before and after 30 days of degradation are shown in Figure 7(a) and compared with the ^{1}H NMR spectra of pristine and degraded $DLL_{17}DV_{66}DLL_{17}$. The representative peaks of the D,L-lactide and δ-valerolactone segments are assigned for the pristine and degraded samples, as shown in Figure 7(a). It is apparent from the ^{1}H NMR spectra that the signals for methine protons (A) at δ = 5.1 ppm and methyl protons (B) at δ = 1.5 ppm for the D,L-lactide block almost disappeared after 30 days of degradation similar to the observations made for $DLL_{17}DV_{66}DLL_{17}$. To determine the loss of D,L-lactide quantitatively, the characteristic peak

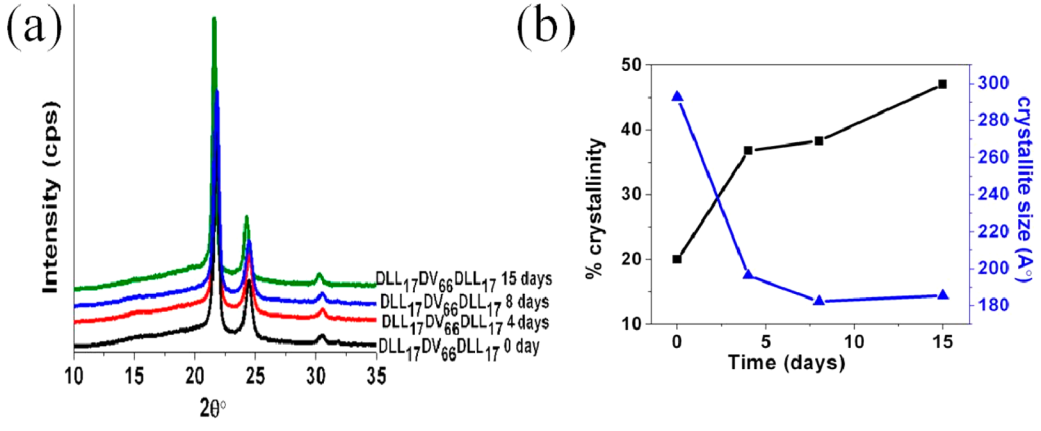

Figure 6. (a) Wide angle X-ray diffraction curves. (b) Plot of % crystallinity and crystallite size for $DLL_{17}DV_{66}DLL_{17}$ after degradation in 20 mM PBS (pH 7.4) at different time intervals.

DOI: 10.1021/acssuschemeng.5b00121
ACS Sustainable Chem. Eng. 2015, 3, 1381−1393

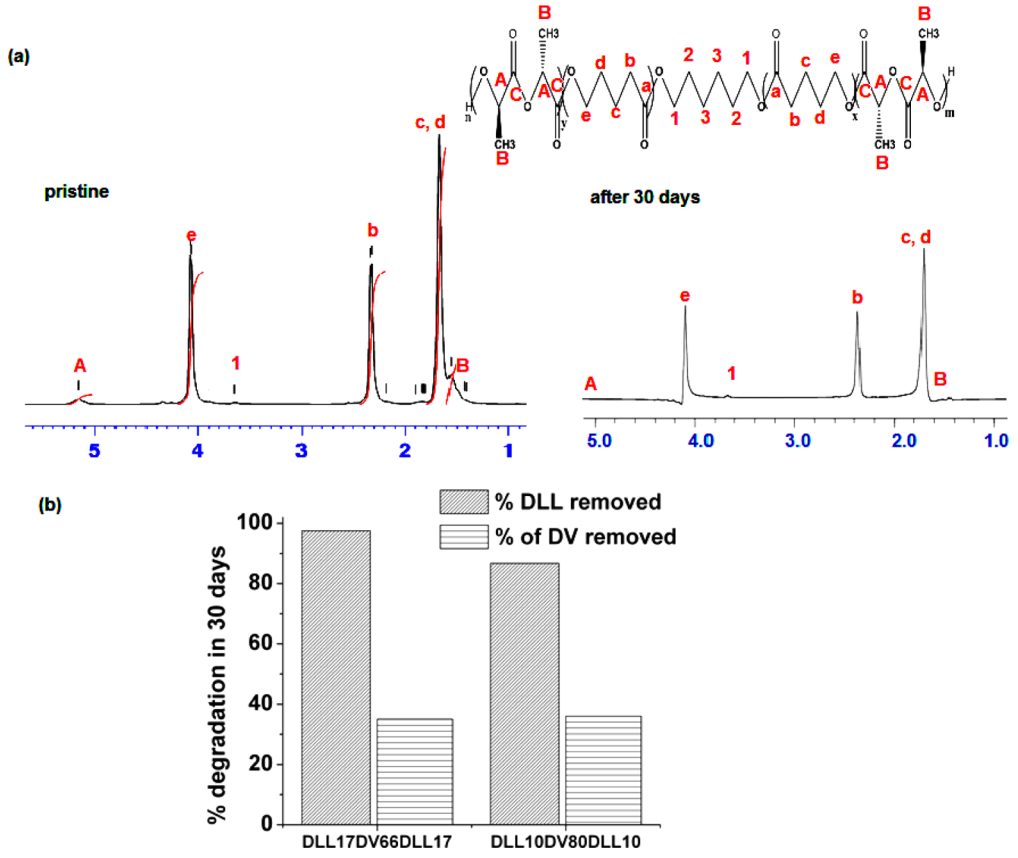

Figure 7. (a) ^{1}H NMR spectra of pristine $DLL_{10}DV_{80}DLL_{10}$ and the sample after 30 days of degradation and (b) the percentage of D,L-lactide and δ-valerolactone degradation calculated from ^{1}H NMR spectra of $DLL_{10}DV_{80}DLL_{10}$ and $DLL_{17}DV_{66}DLL_{17}$ in 20 mM PBS (pH 7.4) after 30 days.

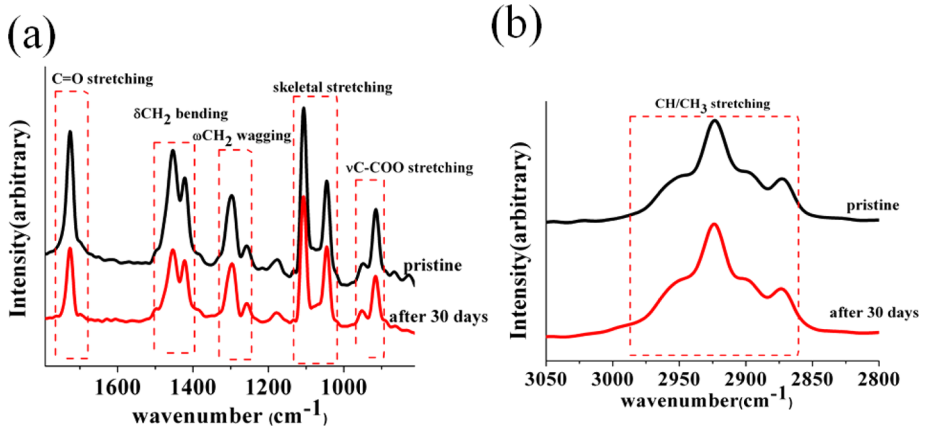

Figure 8. Raman spectra of $DLL_{10}DV_{80}DLL_{10}$ before and after 30 days of degradation in 20 mM PBS (pH 7.4) at (a) 800−1800 cm^{-1} and (b) 2800−3050 cm^{-1}.

intensities of D,L-lactide (δ = 5.1 ppm (A) for methine protons) and δ-valerolactone (δ = 4.2 ppm (e) for methylene protons adjacent to acyl oxygen) were analyzed for the samples both before and after 30 days of degradation. Degradation of both the of the segments is plotted for each sample in Figure 7b. For $DLL_{17}DV_{66}DLL_{17}$, the percent degradation of the molecular weight of D,L-lactide in 30 days was ~97%, which was higher than that for $DLL_{10}DV_{80}DLL_{10}$ (86.7%), as calculated from the corresponding ^{1}H NMR spectra. The percent degradation of the molecular weight for the δ-valerolactone block in $DLL_{17}DV_{66}DLL_{17}$ and $DLL_{10}DV_{80}DLL_{10}$ was in the range of 35%. The initial molecular weights of $DLL_{10}DV_{80}DLL_{10}$ and $DLL_{17}DV_{66}DLL_{17}$ were similar, but the D,L-lactide fraction in $DLL_{17}DV_{66}DLL_{17}$ was higher than that of $DLL_{10}DV_{80}DLL_{10}$. Because of the amorphous nature of the D,L-lactide block, the crystallinity of $DLL_{17}DV_{66}DLL_{17}$ (20%) reduced compared to that of $DLL_{10}DV_{80}DLL_{10}$ (24%).[25] Thus, $DLL_{17}DV_{66}DLL_{17}$ exhibited higher degradation compared to $DLL_{10}DV_{80}DLL_{10}$. The chromatogram of $DLL_{10}DV_{80}DLL_{10}$ (Figure S3b, Supporting Information) shifted toward a longer retention time with a multimodal distribution after 30 days. The appearance of a multimodal distribution along with a higher increase in PDI (Figure S6c, Supporting Information) can be justified by the formation of different polymers having different

DOI: 10.1021/acssuschemeng.5b00121
ACS Sustainable Chem. Eng. 2015, 3, 1381−1393

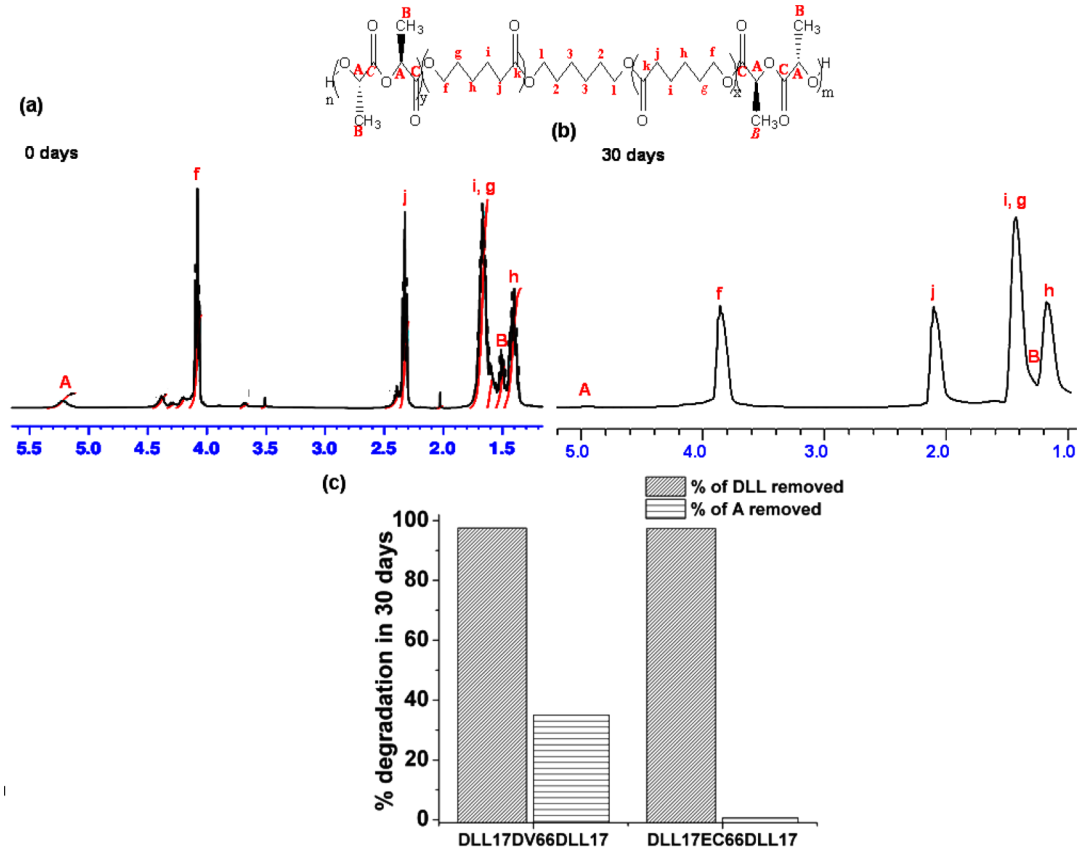

Figure 9. ^{1}H NMR spectra of (a) pristine $DLL_{17}EC_{66}DLL_{17}$ and (b) $DLL_{17}EC_{66}DLL_{17}$ after 30 days of degradation, and (c) the percentage of D,L-lactide segment and A segment degradation calculated from the ^{1}H NMR spectra of $DLL_{17}EC_{66}DLL_{17}$ and $DLL_{17}DV_{66}DLL_{17}$ in 20 mM PBS (pH 7.4) after 30 days.

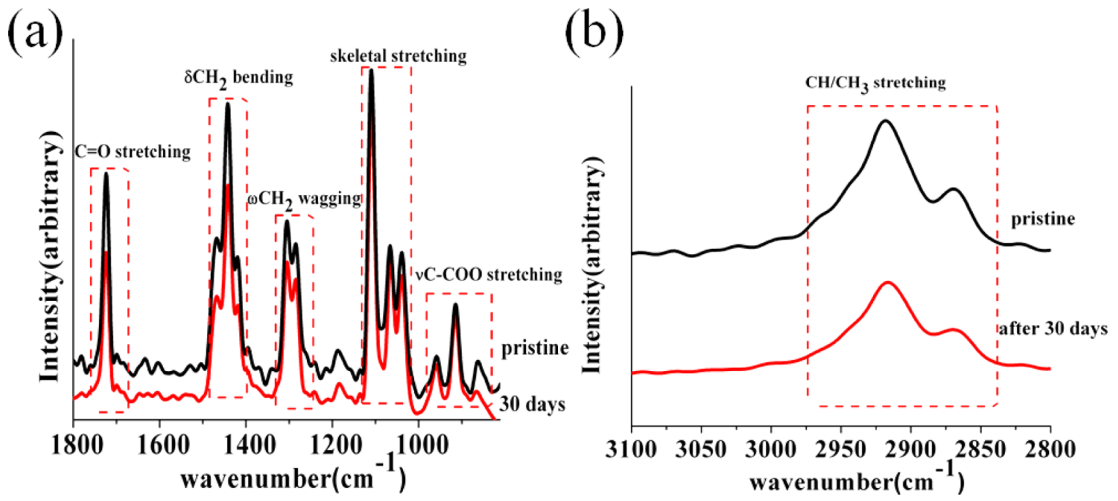

Figure 10. Raman spectra of $DLL_{17}EC_{66}DLL_{17}$ for pristine and after 30 days degradation in 20 mM PBS (pH 7.4) at (a) 800−1800 cm^{-1} and (b) 2800−3000 cm^{-1}.

molecular weights (i.e. the chain scission of polyester linkages may generate homopolymers or oligomers of D,L-lactide, δ-valerolactone, or their triblock). These results are also consistent with the weight loss and water uptake profile (Figure S6, Supporting Information).

Raman spectra for pristine and degraded $DLL_{10}DV_{80}DLL_{10}$ sample are shown in Figure 8. Both of the spectra contained representative signals for C═O stretching at 1725 cm^{-1}, δ −CH_2 bending at 1453 and 1419 cm^{-1}, ω-CH_2 wagging at 1300 and 1257 cm^{-1}, skeletal stretching at 1106 and 1050 cm^{-1}, υC−COO stretching at 950, 915, and 868 cm^{-1}, and CH/CH_3 stretching in the region of 2860−2976 cm^{-1}. The decrease in intensity of the signals after 30 days supported degradation of the sample. The signal at 868 cm^{-1} for υC−COO stretching of the DLL segment completely disappeared after 30 days, certifying removal of the DLL segment from the system, which was also evident from ^{1}H NMR analysis. The peak area analysis of the C═O region indicated that, during the

DOI: 10.1021/acssuschemeng.5b00121
ACS Sustainable Chem. Eng. 2015, 3, 1381−1393

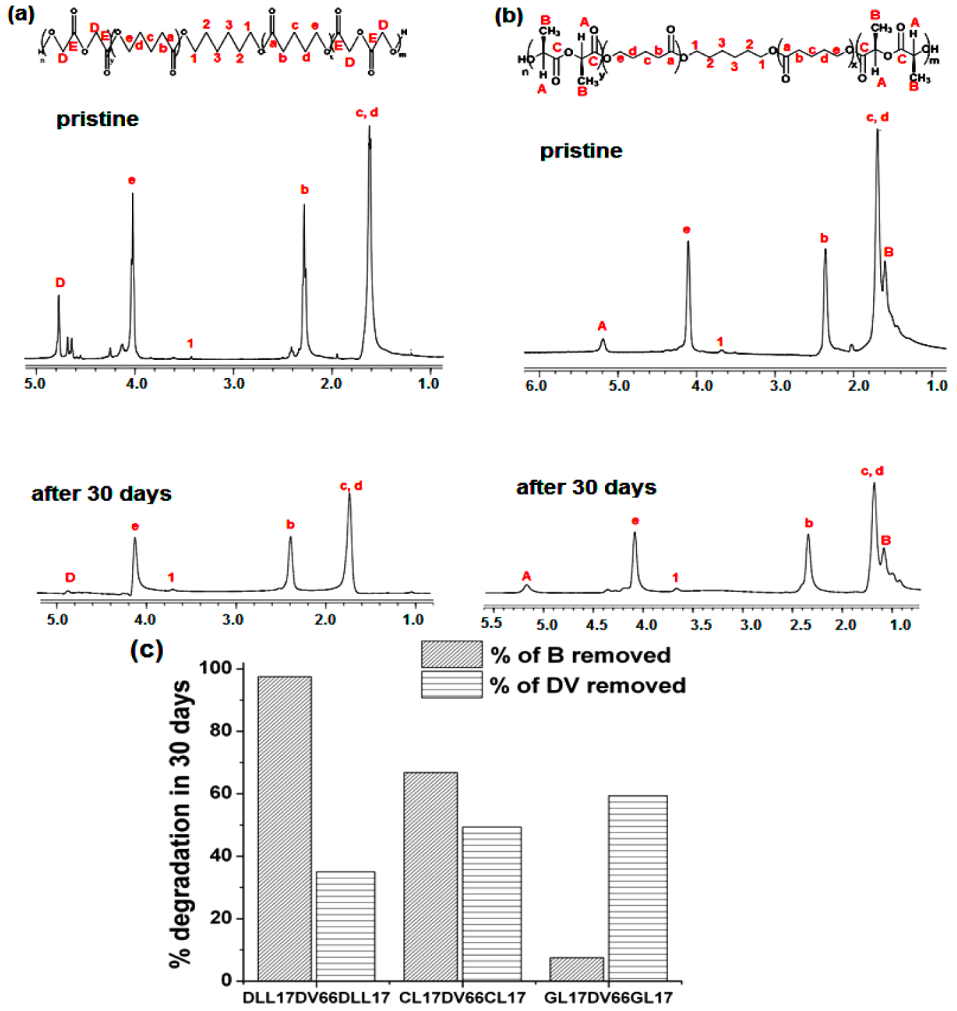

Figure 11. ^{1}H NMR spectra of (a)$GL_{17}DV_{66}GL_{17}$ for pristine and after 30 days of degradation, (b)$CL_{17}DV_{66}CL_{17}$ for pristine and after 30 days of degradation, and (c) percentage of B segment and δ-valerolactone degradation calculated from ^{1}H NMR spectra of $CL_{17}DV_{66}CL_{17}$, $GL_{17}DV_{66}GL_{17}$, and $DLL_{17}DV_{66}DLL_{17}$ in 20 mM PBS (pH 7.4) after 30 days.

30 days, 44% of the ester linkages broke down, which was less than that observed for $DLL_{17}DV_{66}DLL$. The intensity of the CH/CH_3 stretching region decreased by 18% after 30 days of degradation.

Composition Variation. *A-block Variation.* Figure 9 shows the biodegradation of the triblocks when the middle segment was changed to poly ε-caprolactone ($DLL_{17}EC_{66}DLL_{17}$) in place of δ-valerolactone ($DLL_{17}DV_{66}DLL_{17}$). The representative peaks for ε-caprolactone showed an upfield shift of degradation compared to the pristine one after 30 days (i.e., the methylene protons (f) attached to acyl oxygen shifted to 3.8 from 4.1 ppm, the signal for methylene protons (j) adjacent to carbonyl carbon moved to 2 from 2.4 ppm, and the three internal methylene protons (g, h, i) assigned in the region of 1.5−1.6 ppm changed to the region 1.3−1.4 ppm. The intensity of the methine proton (A) and methyl protons (B) of the D,L-lactide segment almost disappeared after 30 days of degradation. Quantitatively, more than 90% of the D,L-lactide block in $DLL_{17}EC_{66}DLL_{17}$ degraded within the 30 day time interval. The ^{1}H NMR spectra of $DLL_{17}EC_{66}DLL_{17}$ further revealed that, compared to the poly δ-valerolactone block in $DLL_{17}DV_{66}DLL_{17}$, the poly ε-caprolactone degraded much less with only 0.64% degradation in 30 days compared to 35% degradation of the δ-valerolactone segment in the same time interval. This is also apparent from Figure S3 in the Supporting Information. $DLL_{17}EC_{66}DLL_{17}$ had lower bulk weight loss and less water uptake compared to that of $DLL_{17}DV_{66}DLL_{17}$ (Figure S6, Supporting Information), which was justified by the crystallinity of $DLL_{17}EC_{66}DLL_{17}$ (33%) being higher than that of $DLL_{17}DV_{66}DLL_{17}$ (20%) and made the copolymer more stable against degradation.

Raman spectra of $DLL_{17}EC_{66}DLL_{17}$ pristine and degraded samples are shown in Figure 10, which represent the signals for C═O stretching at 1723 cm^{-1}, multiple peaks for δ-CH_2 bending at 1414, 1444, and 1468 cm^{-1}, two peaks for ω-CH_2 wagging at 1300 and 1283 cm^{-1}, signals for skeletal stretching at 1038, 1066, and 1109 cm^{-1}, and three peaks for υC−COO stretching at 862, 914, and 959 cm^{-1}. The region between 2836 and 2984 cm^{-1} corresponds to CH/CH_3 stretching, which was also decreased after 30 days. The intensity of all of the other signals also decreased after 30 days. The intensity of the ester carbonyl (C═O) at 1723 cm^{-1} decreased by 29% during the 30 day time period, which was lower than that observed for $DLL_{17}DV_{66}DLL_{17}$ (55%). This further justified the fact that chain scission by cleavage of ester bonds occurred in $DLL_{17}DV_{66}DLL_{17}$ to a greater extent than that of $DLL_{17}EC_{66}DLL_{17}$. The middle ε-caprolactone segment having lower biodegradability than the δ-valerolactone segment is due

DOI: 10.1021/acssuschemeng.5b00121
ACS Sustainable Chem. Eng. 2015, 3, 1381−1393

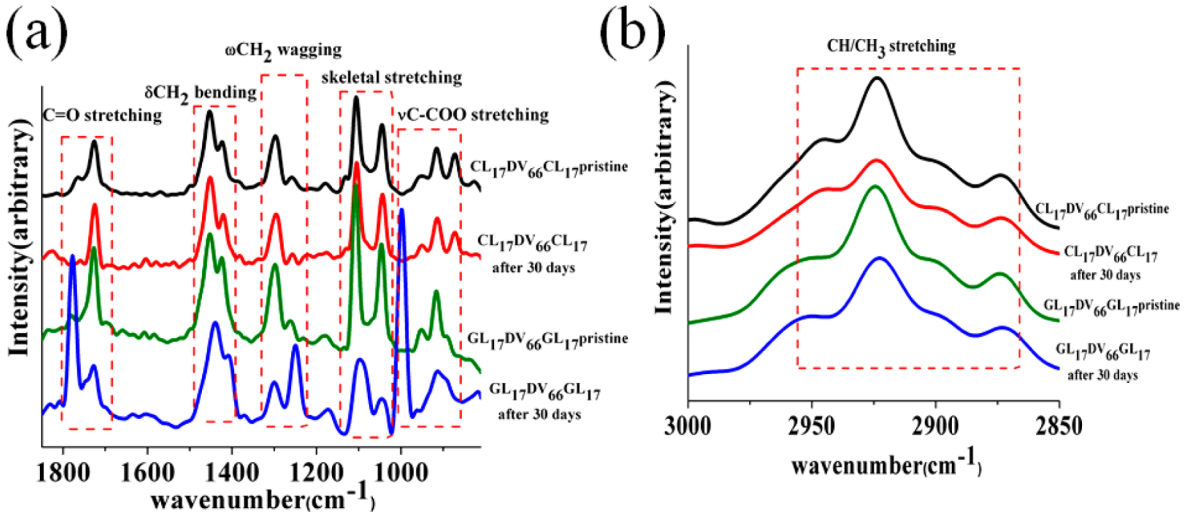

Figure 12. Raman spectra of $CL_{17}DV_{66}CL_{17}$ and $GL_{17}DV_{66}GL_{17}$ for pristine and after 30 days of degradation in 20 mM PBS (pH 7.4) at (a) 800−1800 cm^{-1} and (b) 2850−3000 cm^{-1}.

to its higher crystallinity, which makes it more hydrophobic in nature. The lower biodegradability of poly ε-caprolactone has previously been reported in the literature.[31,32]

B-block Variation. The ^1H NMR spectra (Figure 11) of $CL_{17}DV_{66}CL_{17}$ and $GL_{17}DV_{66}GL_{17}$, both triblocks with δ-valerolactone as the mid segment, contained the signals of the constituents. The presence of the δ-valerolactone segment is assigned by the representative signals, such as at δ = 4.2 ppm for methylene protons (e) adjacent to acyl oxygen, at δ = 2.3 ppm for methylene protons attached to carbonyl group (b), and two internal methylene protons (c, d) at 1.7 ppm, as discussed earlier. The terminal segment was altered as cis-lactide in $CL_{17}DV_{66}CL_{17}$ and as glycolide in $GL_{17}DV_{66}GL_{17}$. The signals for cis-lactide appeared in the same region as seen for D,L-lactide (i.e., at δ = 5.1 ppm for methine protons (A) and at δ = 1.6 ppm for methyl protons (B)). The incorporation of the glycolide segment was supported by the multiple signals in the region δ = 4.8 ppm for methylene protons (D) in between acyl oxygen and carbonyl carbon. The intensity of the representative protons decreased after degradation, as evident from the spectra of $CL_{17}DV_{66}CL_{17}$ and $GL_{17}DV_{66}GL_{17}$. The intensities of the characteristic protons in the terminal B segment and δ-valerolactone segment for pristine and degraded samples were analyzed to determine the molecular weight of each segment, and the results were compared with the degradation of $DLL_{17}DV_{66}DLL_{17}$. Maximum degradation of the B segment occurred for D,L-lactide in $DLL_{17}DV_{66}DLL_{17}$ (97%), followed by cis-lactide in $CL_{17}DV_{66}CL_{17}$ (67%), and glycolide in $GL_{17}DV_{66}GL_{17}$ (7.5%). The middle δ-valerolactone segment degraded for $GL_{17}DV_{66}GL_{17}$ (59%) the most compared to that of $CL_{17}DV_{66}CL_{17}$ (49%) and $DLL_{17}DV_{66}DLL_{17}$ (35%). Cis-lactide and glycolide possess more ordered stereochemistry than D,L-lactide, making them more stable against degradation. The mass loss associated with bulk weight loss and water uptake values (shown in Figure S6, Supporting Information) were also highest for $DLL_{17}DV_{66}DLL_{17}$. The molecular weight distribution curves displayed multimodal distribution for $CL_{17}DV_{66}CL_{17}$, indicating the remnant might contain the homopolymers or oligomers of cis-lactide, δ-valerolactone, or their triblock, and the change in PDI (Figure S6, Supporting Information) after degradation for $CL_{17}DV_{66}CL_{17}$ and $GL_{17}DV_{66}GL_{17}$ was higher than that for $DLL_{17}DV_{66}DLL_{17}$.

Raman spectra of $GL_{17}DV_{66}GL_{17}$ and $CL_{17}DV_{66}CL_{17}$ for pristine and degraded samples are presented in Figure 12. For $CL_{17}DV_{66}CL_{17}$, the C═O stretching signal at 1726 cm^{-1} was associated with a weak signal at 1766 cm^{-1}, attributed to C═O stretching for the CL segment (cis-lactide). This signal at 1766 cm^{-1} weakened after 30 days of degradation, and the peak at 1726 cm^{-1} became sharper. This observation supported degradation of the cis-lactide segment. The other characteristic signals were as follows: at 1422 and 1453 cm^{-1} for δ $-CH_2$ bending, at 1256 and 1296 cm^{-1} for ω-CH_2 wagging, at 1045 and 1106 cm^{-1} for skeletal stretching, at 872, 914, and 952 cm^{-1} for υC−COO stretching, and at 2855−2996 cm^{-1} with a broad region of multiple peaks for CH/CH_3 stretching. Their intensities also decreased with degradation. The Raman spectrum of $GL_{17}DV_{66}GL_{17}$ after 30 days of degradation was significantly different from that of the pristine sample. The C═O stretching region was designated by a strong peak at 1724 cm^{-1} associated with a weak signal at 1780 cm^{-1}. The peak at 1724 cm^{-1} was for C═O stretching of the DV segment, and that at 1780 cm^{-1} was for the GL segment. However, after 30 days of degradation, the peak at 1776 cm^{-1} became stronger in intensity than the peak at 1724 cm^{-1}. The two peaks at 1425 and 1450 cm^{-1}, assigned for δ-CH_2 bending, shifted to 1406 and 1439 cm^{-1} after degradation. Initially, for ω-CH_2 wagging, two peaks were noticed at 1259 and 1298 cm^{-1} with higher intensity than the former. But after 30 days, the peak at 1259 cm^{-1} moved to 1247 cm^{-1}, and its intensity was higher than that at 1298 cm^{-1}. The skeletal stretching region of δ-valerolactone was defined by two peaks at 1107 and 1046 cm^{-1}, whose intensity decreased in the spectrum after 30 days of degradation. Multiple signals at 888, 916, and 952 cm^{-1} were observed for υC−COO stretching for the pristine one. After 30 days of degradation, a strong band at 996 cm^{-1} was displayed with a broad peak at 916 cm^{-1}. The peak at 888 cm^{-1} accounted for the amorphousness of the polyglycolide segment, whereas the appearance of stronger peaks at 1776, 1247, and 996 cm^{-1} justified the presence of crystalline Raman bands of the polyglycolide segment.[33] In the pristine sample, signals were detected for the amorphous regions present in the polyglycolide segment (GL); during the degradation, the

DOI: 10.1021/acssuschemeng.5b00121
ACS Sustainable Chem. Eng. 2015, 3, 1381−1393

amorphous regions were removed preferentially, whereas the crystalline domains remained unchanged as evident by the Raman spectrum after 30 days of degradation. The crystallinity of polyglycolide was retained after 30 days of degradation; no such phenomenon was evident for $DLL_{17}DV_{66}DLL_{17}$ or $CL_{17}DV_{66}CL_{17}$. The retention of crystallinity for the polyglycolide segment was due to its structural symmetry.

Degradation Rate. The degradation rate after 30 days for all the copolymers is given in Table 3. The rate of degradation

Table 3. Degradation Rate Calculated from NMR and Weight Loss for All of the Terpolymers

sample	degradation rate (from loss of M_w from ^{1}H NMR)	degradation rate (gravimetric weight loss)
$DLL_{17}DV_{66}DLL_{17}$	1.6	1.05
$DLL_{10}DV_{80}DLL_{10}$	1.35	0.89
$DLL_{17}EC_{66}DLL_{17}$	0.83	0.26
$CL_{17}DV_{66}CL_{17}$	1.50	0.76
$GL_{17}DV_{66}GL_{17}$	1.58	0.67

estimated from ^{1}H NMR was compared with the degradation rate determined from loss of material gravimetrically. $DLL_{17}DV_{66}DLL_{17}$ exhibited a higher rate of degradation than $DLL_{10}DV_{80}DLL_{10}$ and $DLL_{17}EC_{66}DLL_{17}$, as evident from both the rate of degradation, which has already been justified by their difference in crystallinity introduced by their chemical composition (i.e., as the amount of amorphous DLL was lower in $DLL_{10}DV_{80}DLL_{10}$, the rate automatically dropped). EC was more stable than DV due to its higher crystalline nature, which increased its hydrophobicity. As a result, the degradation of $DLL_{17}EC_{66}DLL_{17}$ was much slower than that of $DLL_{17}DV_{66}DLL_{17}$. For both $CL_{17}DV_{66}CL_{17}$ and $GL_{17}DV_{66}GL_{17}$, the degradation rate, measured by the change in molecular weight from ^{1}H NMR, was marginally lower than that of $DLL_{17}DV_{66}DLL_{17}$, but the degradation rate determined from loss of material was highest for $DLL_{17}DV_{66}DLL_{17}$, followed by $CL_{17}DV_{66}CL_{17}$ and $GL_{17}DV_{66}GL_{17}$. In ^{1}H NMR (Figure 11), the degradation of the CL and GL segments was less than that of DLL, which is in line with the rate of weight loss for the corresponding triblocks.

CONCLUSIONS

The lactone-based terpolymers immersed in 20 mM PBS (pH 7.4) over a time period of 30 days were shown to undergo gradual degradation and thus a gradual elimination of byproducts over time. Its degradation profile was investigated by Raman and NMR spectroscopies. The molecular weight of the δ-valerolactone segment analyzed by ^{1}H NMR exhibited a gradual decrease over time, whereas the molecular weight of the D,L-lactide segment rapidly decreased up to 15 days. The lactide/lactone weight ratio was reduced from 22:78 to 1:99 after 30 days of degradation with disappearance of the characteristic signals of D,L-lactide. The presence of D,L-lactide introduced amorphousness into the semicrystalline polymer, and a decrease in the D,L-lactide ratio reduced the amorphous nature of the triblock, making the triblock more resistant toward degradation. In GPC, the presence of multimodal curves after degradation signified the presence of homopolymers, oligomers, and copolymers of constituting blocks. Exchanging the middle block with poly ε-caprolactone in place of poly δ-valerolactone showed an upfield shift of the characteristic protons of ε-caprolactone and only 0.64% degradation in 30 days, as analyzed from the peak intensities of ^{1}H NMR. Replacement of the D,L-lactide terminal segment by cis-lactide or glycolide also lowered the degradation of the triblock, as evident from ^{1}H NMR spectra. In Raman analysis, the disappearance of signal at 870 cm^{-1} assigned for υC−COO stretching for DLL segment confirmed the removal of the D,L-lactide segment from the system. Peak area analysis of the C═O region revealed that higher ester bond cleavage (55%) occurred in the higher D,L-lactide containing triblock compared to other triblocks. The lower biodegradation for the triblock with ε-caprolactone as the middle segment was also evident from the Raman spectra showing a 29% decrease in C═O stretching after degradation. The Raman spectrum of the glycolide-containing triblock displayed crystalline Raman bands with the appearance of strong peaks at 1776, 1247, and 996 cm^{-1} after a degradation period of 30 days. The hydrolytic degradation of δ-valerolactone- and D,L-lactide-containing triblock was further justified by DSC with sharpening of the melting peak and a drastic increase in the ΔH_m value from 19 J/g to 100 J/g and from SEM demonstrating both surface and internal degradation after 30 days.

ASSOCIATED CONTENT

Supporting Information

FTIR spectra of the triblocks at different time intervals of degradation in Figure S1; FTIR spectra of aliquots after degradation in Figure S2; molecular weight distribution curves for all of the copolymers before and after degradation in Figure S3; DSC thermograms in Figure S4; SEM photographs of surface morphology of the triblocks before and after degradation in Figure S5; and change of weight loss, water uptake, and PDI with time for all of the copolymers in Figure S6. The Supporting Information is available free of charge on the ACS Publications website at DOI: 10.1021/acssuschemeng.5b00121.

AUTHOR INFORMATION

Corresponding Author

*Phone: +91-3222-283180. Fax: + 91-3222-220312. E-mail: anilkb@rtc.iitkgp.ernet.in.

Notes

The authors declare no competing financial interest.

REFERENCES

(1) Gross, R. A.; Kalra, B. Biodegradable Polymers for the Environment. *Science* **2002**, *297*, 803−807.

(2) Andriano, K. P.; Pohjonen, T.; Tormala, P. Processing and Characterization of Absorbable Polylactide Polymers for Use in Surgical Implants. *J. Appl. Biomater.* **1994**, *5*, 133−140.

(3) Wischke, C.; Tripodo, G.; Choi, N.-Y.; Lendlein, A. Hydrolytic Degradation Behavior of Poly(rac-lactide)-block-poly(propylene glycol)-block-poly(rac-lactide) Dimethacrylate Derived Networks Designed for Biomedical Applications. *Macromol. Biosci.* **2011**, *11*, 1637−1646.

(4) Bini, T. B.; Gao, S.; Xu, X.; Wang, S.; Ramakrishna, S.; Leong, K. W. Peripheral Nerve Regeneration by Microbraided Poly(L-lactide-co-glycolide) Biodegradable Polymer Fibers. *J. Biomed. Mater. Res., Part A* **2004**, *68*, 286−295.

(5) Woodruff, M. A.; Hutmacher, D. W. The Return of a Forgotten Polymer—Polycaprolactone in the 21st century. *Prog. Polym. Sci.* **2010**, *35*, 1217−1256.

(6) Huang, M.-H.; Li, S.; Vert, M. Synthesis and Degradation of PLA−PCL−PLA Triblock Copolymer Prepared by Successive

DOI: 10.1021/acssuschemeng.5b00121
ACS Sustainable Chem. Eng. 2015, 3, 1381−1393

Polymerization of ε-caprolactone and D,L-lactide. *Polymer* **2004**, *45*, 8675−8681.
(7) Wanamaker, C. L.; Tolman, W. B.; Hillmyer, M. A. Hydrolytic Degradation Behavior of a Renewable Thermoplastic Elastomer. *Biomacromolecules* **2009**, *10*, 443−448.
(8) George, K. A.; Chirila, T. V.; Wentrup-Byrne, E. Effects of Crosslink Density on Hydrolytic Degradation of Poly(L-lactide)-based Networks. *Polym. Degrad. Stab.* **2012**, *97*, 964−971.
(9) Tsuji, H. Poly(lactide) Stereocomplexes: Formation, Structure, Properties, Degradation, and Applications. *Macromol. Biosci.* **2005**, *5*, 569−597.
(10) Malin, M.; Hiljanen-Vainio, M.; Karjalainen, T.; Seppälä, J. Biodegradable Lactone Copolymers. II. Hydrolytic Study of ε-caprolactone and Lactide Copolymers. *J. Appl. Polym. Sci.* **1996**, *59*, 1289−1298.
(11) Panyam, J.; Dali, M. M.; Sahoo, S. K. Polymer Degradation and In vitro Release of a Model Protein from Poly(D,L-lactide-co-glycolide) Nano- and Microparticles. *J. Controlled Release* **2003**, *92*, 173−187.
(12) Vert, M.; Mauduit, J.; Li, S. Biodegradation of PLA/GA Polymers: Increasing Complexity. *Biomaterials* **1994**, *15*, 1209−1213.
(13) Nair, L. S.; Laurencin, C. T. Biodegradable Polymers as Biomaterials. *Prog. Polym. Sci.* **2007**, *32*, 762−798.
(14) Liu, F.; Zhao, Z.; Yang, J.; Wei, J.; Li, S. Enzyme-catalyzed Degradation of Poly(L-lactide)/Poly(ε-caprolactone) Diblock, Triblock and Four-armed Copolymers. *Polym. Degrad. Stab.* **2009**, *94*, 227−233.
(15) Lee, S. H.; Kim, B. S.; Kim, S. H. Elastic Biodegradable Poly(glycolide-co-caprolactone) Scaffold for Tissue Engineering. *J. Biomed. Mater. Res., Part A* **2003**, *66*, 29−37.
(16) Wong, H. M.; Wang, J. J.; Wang, C.-H. In Vitro Sustained Release of Human Immunoglobulin G from Biodegradable Microspheres. *Ind. Eng. Chem. Res.* **2001**, *40*, 933−948.
(17) Romero, G.; Ochoteco, O.; Sanz, D. J.; Estrela-Lopis, I.; Donath, E.; Moya, S. E. Poly(Lactide-co-Glycolide) Nanoparticles, Layer by Layer Engineered for the Sustainable Delivery of AntiTNF-α. *Macromol. Biosci.* **2013**, *13*, 903−912.
(18) Wu, X. S.; Wang, N. Synthesis, Characterization, Biodegradation, and Drug Delivery Application of Biodegradable Lactic/Glycolic Acid Polymers. Part II: Biodegradation. *J. Biomater. Sci. Polym. Ed.* **2001**, *12*, 21−34.
(19) Odent, J.; Raquez, J.-M.; Duquesne, E.; Dubois, P. Random Aliphatic Copolyesters as New Biodegradable Impact Modifiers for Polylactide Materials. *Eur. Polym. J.* **2012**, *48*, 331−340.
(20) Nakayama, A.; Kawasaki, N.; Maeda, Y.; Arvanitoyannis, I.; Aiba, S.; Yamamoto, N. Study of Biodegradability of Poly(δ-valerolactone-co-L-lactide)s. *J. Appl. Polym. Sci.* **1997**, *66*, 741−748.
(21) Bhowmick, A. K.; Rampalli, S.; Gallagher, K.; Seeger, R.; McIntyre, D. The Degradation of Guayule Rubber and the Effect of Resin Components on Degradation at High Temperature. *J. Appl. Polym. Sci.* **1987**, *33*, 1125−1139.
(22) Banik, I.; Bhowmick, A. K.; Raghavan, S. V.; Majali, A. B.; Tikku, V. K. Thermal Degradation Studies of Electron Beam Cured Terpolymeric Fluorocarbon Rubber. *Polym. Degrad. Stab.* **1999**, *63*, 413−421.
(23) Bhowmick, A. K.; Heslop, J.; White, J. R. Effect of Stabilizers in Photodegradation of Thermoplastic Elastomeric Rubber−Polyethylene Blends—a Preliminary Study. *Polym. Degrad. Stab.* **2001**, *74*, 513−521.
(24) Sengupta, R.; Sabharwal, S.; Bhowmick, A. K.; Chaki, T. K. Thermogravimetric Studies on Polyamide-6,6 Modified by Electron Beam Irradiation and by Nanofillers. *Polym. Degrad. Stab.* **2006**, *91*, 1311−1318.
(25) Kasyapi, N.; Bhowmick, A. K. Nanolamellar Triblock of Poly-D,L-lactide−δ-valerolactone−D,L-lactide with Tuneable Glass Transition Temperature and Crystallinity for Use as a Drug-delivery Vesicle. *RSC Adv.* **2014**, *4*, 27439−27451.
(26) Kasyapi, N.; Bhowmick, A. K. Spectroscopic and Morphology Studies of Biodegradable Nanolamellar Lactone Based Triblocks. *J. Phys. Chem. C* **2014**, *118*, 22325−22338.
(27) Göpferich, A. Mechanisms of polymer degradation and erosion. *Biomaterials* **1996**, *17*, 103−114.
(28) Montaudo, G.; Garozzo, D.; Montaudo, M. S.; Puglisi, C.; Samperi, F. Molecular and Structural Characterization of Polydisperse Polymers and Copolymers by Combining MALDI-TOF Mass Spectrometry with GPC Fractionation. *Macromolecules* **1995**, *28*, 7983−7989.
(29) Biela, T.; Duda, A.; Penczek, S. Control of Mn, Mw/Mn, Endgroups, and Kinetics in Living Polymerization of Cyclic Esters. *Macromol. Symp.* **2002**, *183*, 1−10.
(30) Liu, L.; Li, S.; Garreau, H.; Vert, M. Selective Enzymatic Degradations of Poly(L-lactide) and Poly(ε-caprolactone) Blend Films. *Biomacromolecules* **2000**, *1*, 350−359.
(31) Hong, J. H.; Jeon, H. J.; Yoo, J. H.; Yu, W.-R.; Youk, J. H. Synthesis and Characterization of Biodegradable Poly(ε-caprolactone-co-β-butyrolactone)-based Polyurethane. *Polym. Degrad. Stab.* **2007**, *92*, 1186−1192.
(32) Fernández, J.; Larrañaga, A.; Etxeberria, A.; Sarasua, J. R. Tensile Behavior and Dynamic Mechanical Analysis of Novel Poly(lactide/δ-valerolactone) Statistical Copolymers. *J. Mech. Behav. Biomed. Mater.* **2014**, *35*, 39−50.
(33) Kister, G.; Cassanas, G.; Vert, M. Structure and Morphology of Solid Lactide-Glycolide Copolymers from 13C n.m.r., Infra-red and Raman spectroscopy. *Polymer* **1998**, *39*, 3335−3340.

DOI: 10.1021/acssuschemeng.5b00121
ACS Sustainable Chem. Eng. 2015, 3, 1381−1393